Examination of Stochastic Dispersion Theory by MRI in Aperiodic Porous Media

N. C. Irwin and R. A. Greenkorn
School of Chemical Engineering, Purdue University, West Lafayette, IN 47907

S. A. Altobelli
New Mexico Resonance, Albuquerque, NM 87108

J. H. Cushman
Center for Applied Mathematics, Purdue University, West Lafayette, IN 47907

Magnetic resonance imaging techniques were applied to obtain concentration and velocity field measurements during flow in an aperiodic heterogeneous porous medium. These measurements were used to evaluate the applicability of a stochastic perturbation theory and the validity of the assumptions underlying its derivation. A comparison of experimental moment data to the first and second moments of simulated mean concentration distributions showed that the theory did not match the experimental data. While the results showed general agreement, the stochastic model appeared to slightly overpredict the experimentally observed mixing behavior. Discrepancies between experimental and numerical results were attributed to the assumption that triplet correlation terms involving fluctuating velocities and fluctuating concentration are insignificant relative to terms containing doublet cross-correlations. Measured velocity covariances were compared to the velocity covariance determined from the first-order solution to the flow equation. The first-order relation agreed generally with the measured covariance, but did not accurately predict the detailed covariance structure in the aperiodic heterogeneous model.

Introduction

The accurate modeling of flow in porous media has proven challenging, primarily because of the heterogeneous nature of natural porous systems. It has been shown that mixing in heterogeneous systems is scale-dependent (Matheron and de Marsily, 1980; Smith and Schwartz, 1980; Sudicky et al., 1983; Freyburg, 1986; Garabedian et al., 1991; Gelhar et al., 1992). This scale-dependent behavior prevents the use of the classic advection-dispersion equation for the determination of large-scale flow and transport properties in natural systems. As a result, a stochastic approach to modeling has been adopted in recent years (see Dagan, 1989; Cushman, 1990 for exhaustive references). These models have been extensively developed over the last decade and show promise as a predictive technique.

A nonlocal model for conservative chemical transport in heterogeneous porous media has been developed by Deng and coworkers (Deng et al., 1993). Their approach is based on an Eulerian perturbation solution to the stochastic flow model and has been solved in transform space to yield an equation for the prediction of mean concentration. This solution depends on specific assumptions about the nature of the velocity field and on the use of a first-order equation relating the velocity covariance to the covariance of the log-hydraulic conductivity. Thus, by direct measurement of the velocity field, the applicability of the first-order relation and the validity of the stochastic nonlocal model can be examined.

Managnetic resonance imaging (MRI) presents a noninvasive means to obtain specific information about the behavior of the velocity field (such as Caprihan and Fukushima, 1990). MRI flow measurement techniques have been extensively developed over the last two decades and their application to the

Correspondence concerning this article should be addressed to R. A. Greenkorn.

Table 1. Properties of Bead-Size Distributions in Each Section of Aperiodic Heterogeneous Model

Property	Top Section	Middle Section	Bottom Section
U.S. sieve series mesh no.	20–28	35–48	100–115
Bead range (μm)	600–850	300–425	125–150
Porosity	0.339	0.324	0.336
Permeability (Da)	320	53.2	10.3
Pore-size range (μm)	150–200	75–100	25–50

study of flow in porous media has recently become an area of active research (such as Borgia et al., 1990, 1993, 1996). In this study, MRI techniques (Irwin et al., 1998) were applied to obtain concentration and velocity field measurements for the evaluation of the stochastic nonlocal model.

Experiment

MRI techniques were applied to obtain one-dimensional concentration images and two-dimensional velocity images during flow in an aperiodic heterogeneous porous medium (Irwin et al., 1998). Three identical columns, each filled with a homogeneous distribution of unconsolidated spherical glass beads, were threaded together to create a single column with aperiodic heterogeneity. The resulting three-layer model was 183 cm long with an inside diameter of 3.18 cm. The properties of each layer are given in Table 1.

The imaging experiments were performed in a 31.0-cm horizontal bore superconducting magnet at a field of 1.89 T. The Larmor frequency for ^{1}H at this field was 80.34 MHz. The magnet contained actively shielded gradient coils and a high-pass birdcage radio-frequency (rf) probe. Gradient pulses and sampling were controlled using either a Nalorac imaging spectrometer or a Tecmag LIBRA imager. Flow was controlled with a syringe pump assembly that was constructed by attaching an electric stepping motor (motorized shaft) to the piston of a plastic syringe. The motor was driven by a CompuMotor controller and flow rates were adjusted by setting the motor velocity.

Breakthrough experiments were performed by observing the signal buildup created by a step input of water doped with a gadolinium relaxation agent in a model initially saturated with undoped water. The rate of signal buildup was shown to be equivalent to the rate of tracer breakthrough in a conventional breakthrough experiment. A realization of the concentration field was constructed by combining concentration profiles determined from a series of 18 breakthrough images made in 10-cm sections along the length of an aperiodic heterogeneous model. The first two moments of the measured distribution are presented in Figure 1. The discontinuities that are apparent in these profiles are the result of combining data from separate images. This artifact can be avoided in future experiments by making images in overlapping sections. By comparing experimental moment data to the moments of simulated mean concentration distributions, the predictive ability of the stochastic model can be examined.

A modified stimulated-echo technique (Waggoner and Fukushima, 1996) was used to make two-dimensional velocity images during flow in the aperiodic heterogeneous model. Two sets of 18 images were made in 10-cm sections along the

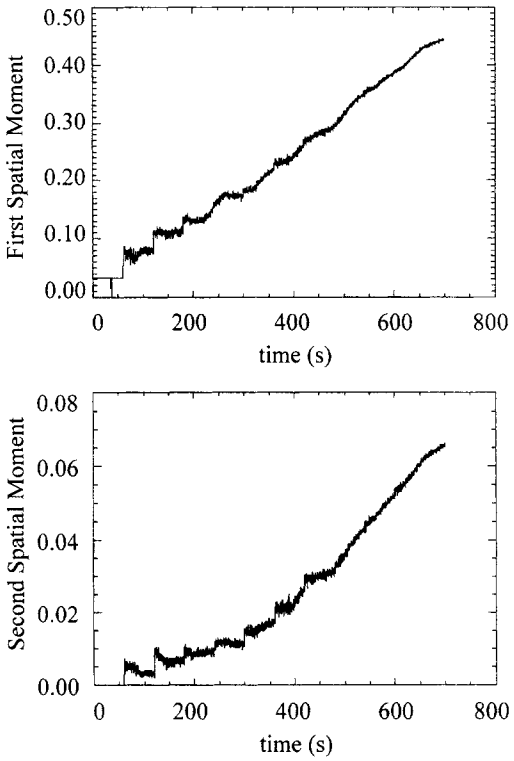

Figure 1. First two spatial moments of measured concentration distribution in the aperiodic heterogeneous model.

length of the model to produce two realizations of the velocity field. A representative set of velocity images from the first realization is presented in Figure 2. The resolution of the images shown in this figure is 0.91 mm in the x-direction, 1.16 mm in the z-direction, with a slice thickness of 5 mm in the y-direction. At this resolution, the measured velocity in each voxel represents an average over 40–1000 beads. It has been argued that resolution below the pore scale is necessary in order to obtain reliable data (Nesbitt et al., 1992). For these experiments, an average measurement over several pores was considered appropriate, since the stochastic model is based on a Darcy-scale or superficial velocity.

Velocity covariance functions were determined from each set of velocity images according to (Wei, 1990):

$$R(u) = \frac{1}{N} \sum_{i=1}^{N-u} (W_i - \overline{W})(W_{i+u} - \overline{W}), \qquad (1)$$

where $\overline{W}$ is the mean of the process, u is the lag at which correlation is estimated, i is the location at which W has been measured, and N is the total number of observations. Estimates of the covariance, $R(u)$, are reliable for values of $N \geq 50$ and $u \leq N/4$ (Box, 1976). All nine components of the velocity covariance tensor:

$$R_{ij} = \begin{bmatrix} R_{xx} & R_{xy} & R_{xz} \\ R_{yx} & R_{yy} & R_{yz} \\ R_{zx} & R_{zy} & R_{zz} \end{bmatrix} \qquad (2)$$

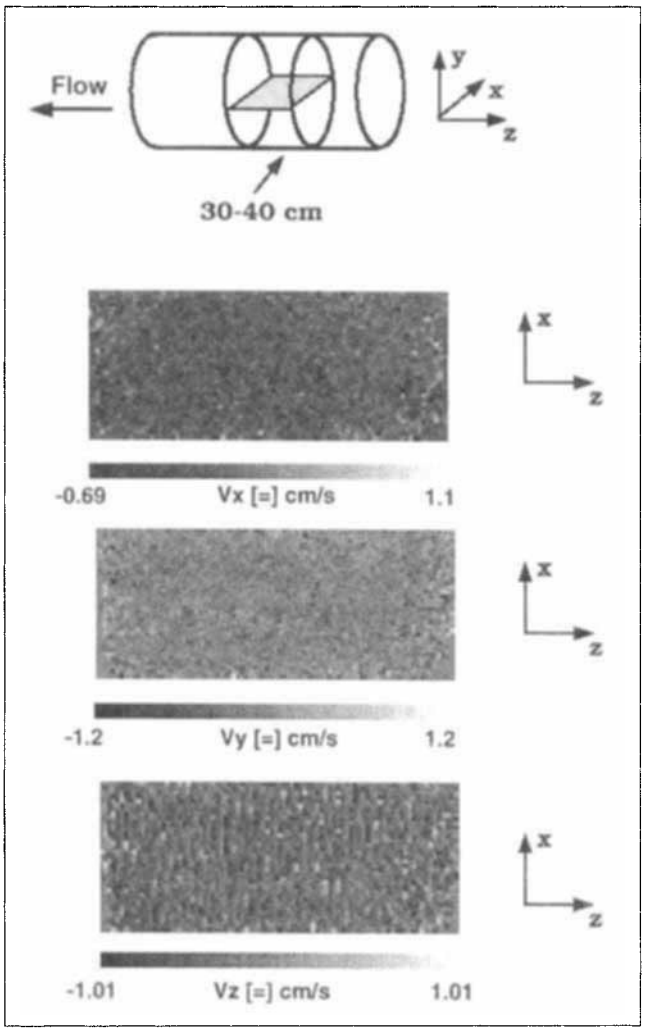

Figure 2. Representative set of images from the first realization of velocity field in the aperiodic heterogeneous model.

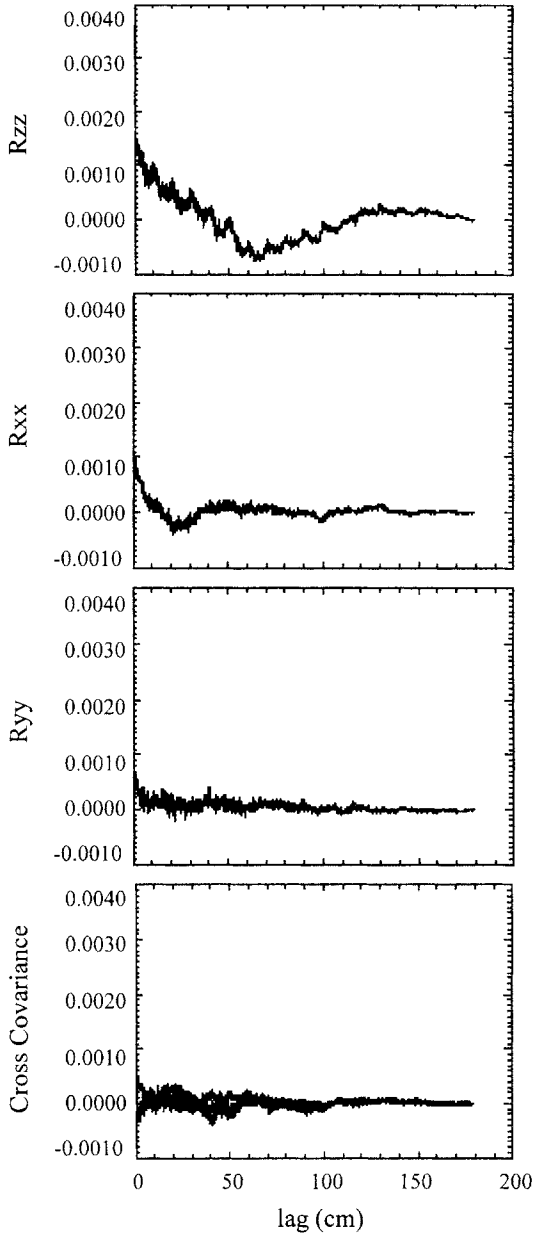

Figure 3. Two-point velocity correlation functions determined from the first realization of velocity field in the aperiodic heterogeneous model.

can be determined from the velocity measurements according to Eq. 1 (note the definition of the coordinate axes in Figure 2). These components are plotted as a function of spatial lag, u, in Figures 3 and 4. For the data shown in these figures, $N = 1548$, therefore, the covariance can be considered reliable for values of $u \leq 387$ (45 cm). Construction of the velocity covariance from measurements of the fluctuating velocity makes it possible to examine the validity of the first-order relation and the applicability of the stochastic transport model.

It is interesting to note that the covariance takes on negative values. This negative correlation reflects the oscillatory behavior of the velocity field. Oscillations about the mean velocity result in correlation between positive and negative velocity fluctuations. Thus, regions in which the velocity is higher than average are affected by regions in which the velocity is lower than average, and vice versa. Although negative velocity fluctuations do not necessarily indicate flow reversal, it should be noted that some negative velocities are evident in the velocity images. The large negative fluctuations, $v = -1$ cm/s, are clearly outliers. These values are likely the result of phase wrapping in the NMR signal. Negative velocity fluctuations on the order of -0.5 cm/s are not outliers and indicate that some recirculation may be occurring near the end of the model. Notwithstanding, these negative velocities are not predominant throughout the velocity profiles or the velocity images, thus, this recirculation may not be significant.

Theory

The stochastic nonlocal model was adapted to the initial condition of the breakthrough imaging experiment:

$$C(x_1 = 0, |x_2| \leq b, t) = C_m \quad t \geq 0, \tag{3}$$

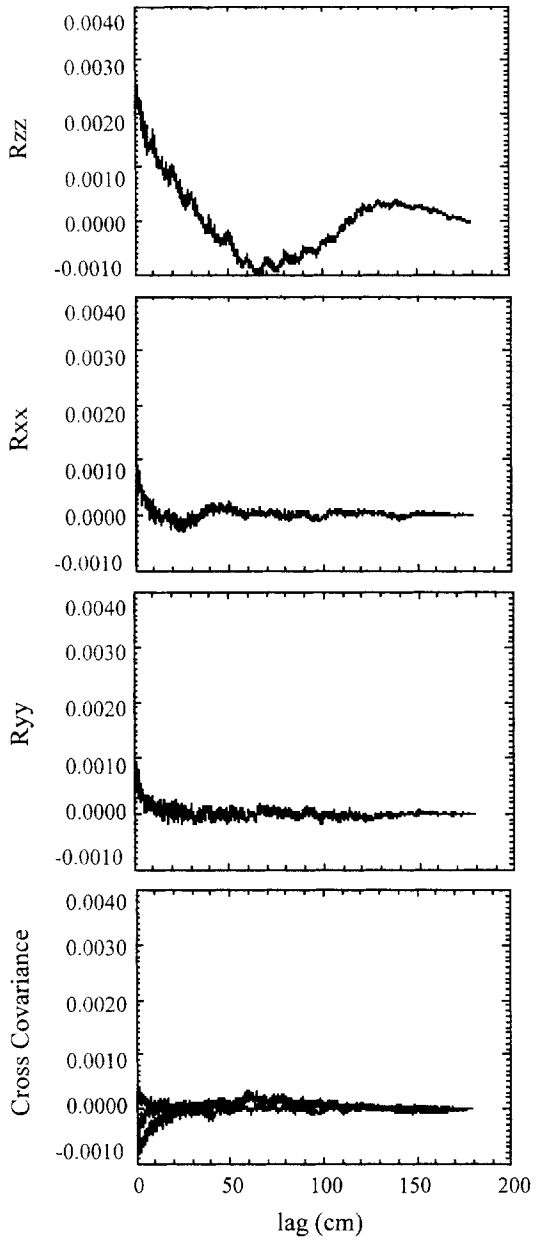

Figure 4. Two-point velocity correlation functions determined from the second realization of velocity field in the aperiodic heterogeneous model.

where C_m is the initial concentration, and b is the radius of the experimental model. For a continuous source, the Darcy scale transport equation is written:

$$\frac{\partial C}{\partial t} + \frac{\partial (V_i C)}{\partial x_i} - \frac{\partial}{\partial x_i}\left(D_{ij}\frac{\partial C}{\partial x_j}\right) = C_0 \cdot H(t), \qquad (4)$$

where

$$C_0 = C_m \Pi\left(\frac{x_2}{2b}\right) \qquad (5)$$

is a rectangle function whose Fourier transform is given by

$$\hat{C}_0(\boldsymbol{k}) = C_m \frac{2\sin(bk_2)}{k_2} \qquad (6)$$

and $H(t)$ is Heaviside's unit step function:

$$H(t) = \begin{cases} 0 & t < 0 \\ 1 & t > 0. \end{cases} \qquad (7)$$

Following the approach outlined by Deng et al. (1993), the mean equation is written:

$$\frac{\partial \overline{C}}{\partial t} + \overline{V}_1 \frac{\partial \overline{C}}{\partial x_1} - D_i \frac{\partial^2 \overline{C}}{\partial x_i^2} = -\frac{\partial \overline{cv_i}}{\partial x_i} + C_0 \cdot H(t). \qquad (8)$$

The mean-removed equation is unchanged:

$$\frac{\partial c}{\partial t} + \overline{V}_1 \frac{\partial c}{\partial x_1} - D_i \frac{\partial^2 c}{\partial x_i^2} = -v_i \frac{\partial \overline{C}}{\partial x_i} - \frac{\partial (v_i c)}{\partial x_i} + \frac{\partial \overline{cv_i}}{\partial x_i}. \qquad (9)$$

Taking Laplace and Fourier transforms, Eqs. 8 and 9 become

$$s\overline{C}^o + ik_1\overline{V}_1\overline{C}^o + D_i k_i^2 \overline{C}^o = -ik_i\overline{cv_i}^o + \frac{\hat{C}_0}{s} \qquad (10)$$

$$sc^o + ik_1\overline{V}_1 c^o + D_i k_i^2 c^o = -\left[v_i \frac{\partial \overline{C}}{\partial x_i}\right]^o - ik_i\left[[v_i c]^o - \overline{cv_i}^o\right]. \qquad (11)$$

Continuing with the analysis as outlined by Deng et al. (1993), the Fourier-space solution for the mean concentration is written:

$$\overline{C}^o = \frac{\hat{C}_0}{s}\left[B^{o-1} + \left(\frac{1}{2\pi}\right)^3 (k_i k_j)\left(B^o *_k \hat{R}_{ij}\right)\right]^{-1}$$

$$= \frac{\hat{C}_0}{s}\left[s + ik_1\overline{V}_1 + D_m k_m^2 + \left(\frac{1}{2\pi}\right)^3 (k_i k_j) \cdot \int_{R^3} \frac{\hat{R}_{ij}(\boldsymbol{k} - \boldsymbol{k}')}{s + ik_1'\overline{V}_1 + D_m k' m^2} dk'\right]^{-1}. \qquad (12)$$

To evaluate Eq. 12, one must know the velocity covariance function, R_{ij}, the initial concentration distribution, C_0, the mean velocity, $\overline{V}_1$, and the local dispersivities. The velocity covariance function is typically obtained using a first-order relation between velocity and log-hydraulic conductivity covariance (Gelhar and Axeness, 1983). By directly measuring R_{ij}, the applicability of this first-order relation and the validity of the stochastic transport model can be examined.

Table 2. Values Assigned to Input Parameters of Numerical Model

Input	Parameter	Assigned Value
Initial concentration	C_m	0.00149 g/cm^3
Radius of experimental model	b	1.59 cm
Mean velocity	$\bar{V}_1$	0.25 cm/s
Longitudinal dispersivity	α_L	0.176 cm
Transverse dispersivity	α_T	0.0587 cm
ln K variance	σ_f^2	0.15
ln K integral scale	$\lambda_1 = \lambda_2 = \lambda$	2.0 cm
Porosity	n	0.33
Geometric mean of conductivity	$K_g = e^{\bar{F}}$	0.0256 cm/s
Mean hydraulic gradient	J	3.22
Velocity covariance	R_{ij}	
Simulation 1	R_{ij}	Eq. 14
Simulation 2	R_{11}	R_{zz} in Fig. 3
	R_{22}	R_{xx} in Fig. 3
	$R_{12} = R_{21}$	R_{zx} in Fig. 3
Simulation 3	R_{11}	R_{zz} in Fig. 4
	R_{22}	R_{xx} in Fig. 4
	$R_{12} = R_{21}$	R_{zx} in Fig. 4
No. of computational nodes	in x_1	120
	in x_2	20
	in t	120

Numerical Modeling

Since the imaging experiments yield results for various quantities that are averages over a slice thickness of 5 mm in the y-direction, two-dimensional simulations (that is, simulations in x and z) of mean concentration were performed for comparison with experimental data. The coordinate axes x and z defined for the imaging experiments correspond to variables x_1 and x_2 in the stochastic transport model. Values assigned to the input parameters of the stochastic nonlocal model are presented in Table 2. Values for the initial concentration, C_m, the radius of the experimental model, b, the mean velocity, V_1, and the porosity, n, are dictated by the constraints of the imaging experiments. The initial concentration is set equal to the concentration of dopant used in the experiment, the mean velocity is defined by the experimental average linear velocity, and the porosity is set equal to the measured porosity of the aperiodic heterogeneous model. The longitudinal dispersivity, α_L, is determined according to:

$$D_L = \alpha_L \bar{V}_1, \tag{13}$$

where D_L is the average longitudinal dispersion in the aperiodic heterogeneous model. The transverse dispersivity, α_T, is set equal to one-third the value assigned to the longitudinal dispersivity (Greenkorn, 1983).

The velocity covariance function is defined in two ways. Simulations are performed using both theoretical and measured velocity covariances as input. Simulation 1 used the velocity covariance determined according to the first-order solution to the flow equation (Gelhar and Axeness, 1983):

$$\hat{R}_{ij}(\boldsymbol{k}) = \left(\frac{JK_g}{n}\right)^2 \left[\delta_{i1} - \frac{k_1 k_i}{k^2}\right]\left[\delta_{j1} - \frac{k_1 k_j}{k^2}\right] \hat{R}_{ff}(\boldsymbol{k}). \tag{14}$$

Simulations 2 and 3 used the measured covariances shown in Figures 3 and 4.

To compute the velocity covariance function using Eq. 14, the geometric mean of the hydraulic conductivity, K_g, the mean hydraulic gradient, J, and the covariance function of the fluctuating log-hydraulic conductivity, R_{ff}, must be known. The geometric mean of the hydraulic conductivity is defined by the series average of the hydraulic conductivity in each layer of the aperiodic heterogeneous model (Greenkorn, 1983):

$$\langle\langle K\rangle\rangle_s = \frac{L}{L_1/K_1 + L_2/K_2 + L_3/K_3}, \tag{15}$$

where L is the length of the aperiodic heterogeneous model, and L_1, L_2, L_3 are the lengths of the individual layers in the model. The mean hydraulic gradient is determined according to

$$J = \frac{n\bar{V}}{\langle\langle K\rangle\rangle_s}, \tag{16}$$

where $\bar{V}$ is the experimental velocity, $\langle\langle K\rangle\rangle_s$ is the series average hydraulic conductivity, and n is the measured porosity. Given the exponential conductivity structure of the aperiodic heterogeneous model, the covariance function of the fluctuating log-hydraulic conductivity is defined:

$$R_{ff}(x) = \sigma_f^2 \exp - \left[\left(x_1^2/\lambda_1^2\right) + \left(x_2^2/\lambda_2^2\right)\right]^{1/2}, \tag{17}$$

where σ_f^2 and $\lambda_1 = \lambda_2 = \lambda$ are the variance and integral scale of the fluctuating log-hydraulic conductivity, respectively. The variance of the fluctuating conductivity is estimated to be of the same magnitude as the variance of the bead-size distributions in each section of the aperiodic heterogeneous model. The integral scale is estimated to be on the order of 50 times the average bead diameter in the aperiodic heterogeneous model.

Results and Discussion

A comparison of the experimental moment data to the first and second moments of the simulated mean concentration is presented in Figure 5. The first, X_1, and second, X_{11}, longitudinal spatial moments were computed according to (Deng et al., 1993):

$$X_{ii} = 1/M \int_{R^2} n x_i^2 \bar{C}\, d\boldsymbol{x} - X_i^2, \tag{18}$$

where

$$X_i = 1/M \int_{R^2} n x_i \bar{C}\, d\boldsymbol{x}, \tag{19}$$

and

$$M = \int_{R^2} n \bar{C}\, d\boldsymbol{x}. \tag{20}$$

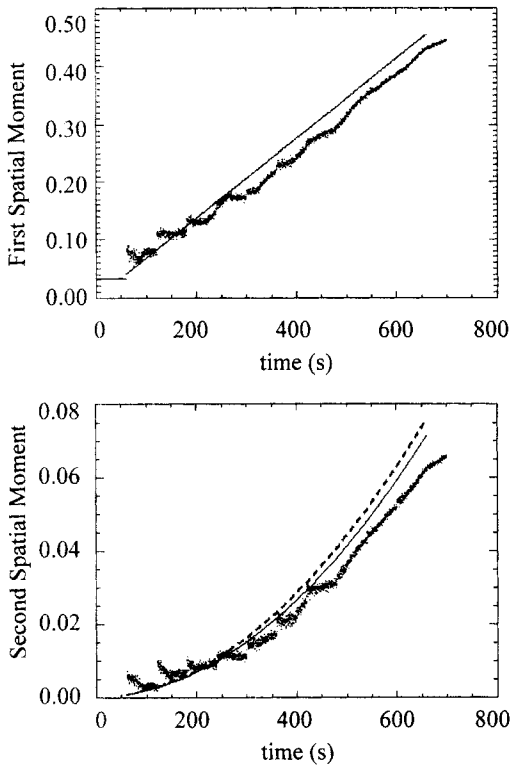

Figure 5. Experimental moment data (data points) vs. moments of simulated mean concentration distributions.

Solid line shows results from simulation based on first-order solution to flow equation (Simulation 1); dotted lines show results from simulations based on measured covariances (Simulations 2 and 3).

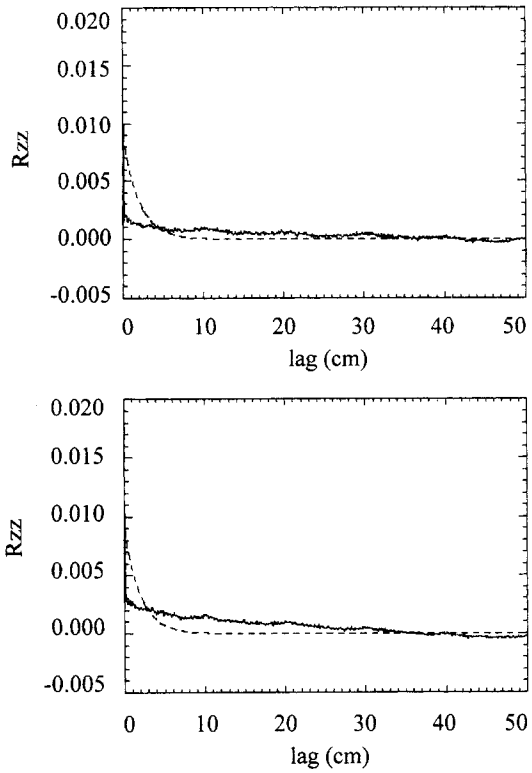

Figure 6. Covariance determined from the Fourier inversion of Eq. 14 (dotted line) vs. the measured covariance (solid line) determined from the first (top figure) and second (bottom figure) realizations of velocity field in the aperiodic heterogeneous model.

Before drawing any conclusions from these results, it should be noted that comparisons were made between ensemble average results and unique experimental realizations. Also, flow and transport processes in a bounded domain were simulated using a model that was developed for an infinite domain. Therefore, small discrepancies were expected between the numerical and experimental results.

Although a set of concentration measurements was not available to compute error bars for the experimental moment data, the measurement error was estimated to be on the order of 10%. Within an error band of $\pm 10\%$, the experimental data show relatively good agreement with the first spatial moments of the simulated mean concentration distributions. However, a comparison of the experimental and theoretical second spatial moments suggests that the simulations do not match the experimentally observed mixing behavior. Even with a variation in the experimental second moment of $\pm 10\%$, the stochastic transport model appears to slightly overpredict the experimental results. It is interesting to note that the simulations, which used measured covariances as input, overpredict the mean concentration more than the simulation, which used the first-order relation between velocity and log-hydraulic conductivity covariance.

To examine the validity of the first-order relation, the measured covariances are compared to the covariance determined from the Fourier inversion of Eq. 14 in Figure 6. Although the first-order relation shows general agreement with the measured covariance, it does not predict the observed negative correlation. While this negative correlation is small with respect to the magnitude of the covariance function, it may have an effect on the mixing behavior. Small negative correlation at the laboratory scale may translate into large negative correlation at the field scale. These velocity measurements suggest that a decaying exponential function may not adequately represent the velocity covariance structure in a heterogeneous system.

Although the first-order relation does not capture the observed negative correlation, higher-order corrections to this relation may improve the agreement between measured and theoretical covariances. The accuracy of the first-order relation has been explored numerically. Deng and Cushman (1995) suggest that for $\sigma_f^2 \ll 1$, the first-order approximation is adequate, but as σ_f^2 approaches unity, higher-order terms become significant. Dagan (1985, 1993) and Thompson and Gelhar (1990), suggest that for isotropic formations, the first-order approximations is accurate for head and velocity covariances up to a log-hydraulic conductivity variance on the order of one. The experimental results shown here suggest that the upper limit on σ_f^2 may be less than unity. These results are in general agreement with the theoretical work of

Hassan (1995), whose Monte Carlo assessment suggests that the first-order approximation may not capture the right covariance structure when $\sigma_f^2 > 0.3$.

While higher-order corrections may explain the observed differences between simulations based on theoretical and measured covariances, they do not explain the discrepancy between the experimental and numerical results. Since the simulations based on measured covariances do not perform as well as those based on theoretical covariances, it is unlikely that incorrect assumptions about the form of the velocity or log-hydraulic conductivity covariance are responsible for differences in the results. Thus, discrepancies between experimental and numerical results must be attributed to the assumptions underlying the development of the stochastic transport model. The main assumption employed by this model is that triplet correlation terms involving fluctuating velocities and fluctuating concentration are neglible compared to the flux terms that contain doublet cross-correlations. While it was not possible to estimate the magnitude of the triplet correlation terms experimentally, these terms may well have a significant effect on the prediction of mean concentration. The relative importance of the triplet correlation terms has been explored numerically by Hassan (1995). The numerical results suggest that these terms are small relative to the convolution flux terms for mildly heterogeneous media.

Summary and Conclusions

Concentration and velocity field measurements in an aperiodic heterogeneous model were used to evaluate the applicability of a stochastic perturbation theory and the assumptions underlying its derivation. A comparison of experimental moment data to the first and second moments of simulated mean concentration distributions showed that the theory did not match the experimental data. While the results showed general agreement, the stochastic model appeared to slightly overpredict the experimentally observed mixing behavior. Discrepancies between experimental and numerical results were attributed to the assumption that triplet correlation terms involving fluctuating velocities and fluctuating concentration are insignificant relative to terms containing doublet cross-correlations.

Measured covariances were compared to the covariance determined from the first-order solution to the flow equation. Although the first-order relation was shown to be in general agreement with the measured covariance, it did not accurately predict the detailed covariance structure. In particular, it was not able to predict the observed negative correlation in the velocity covariance. Notwithstanding, it was concluded that higher-order corrections to this relation may improve the agreement between measured and theoretical velocity covariance.

The experimental results suggest that MRI techniques can provide insight into the contaminant transport problem that cannot be gained using conventional laboratory and field tracer experiments. The detailed spatial information provided by velocity imaging experiments is invaluable to the examination of existing theoretical models. It has been demonstrated that not only can these measurement techniques be used to examine transport theories, they offer avenues for improvement based on experimental evidence of flow behavior.

Acknowledgments

Nancy C. Irwin and Robert A. Greenkorn thank the Showalter Trust and the Purdue Research Foundation for the grants that made this work possible.

Literature Cited

Borgia, G. C., R. J. S. Brown, P. Fantazzini, J. Gore, P. Mansfield, B. Maraviglia, E. Mesini, and L. Sgubini, eds., *Proceedings of the First International Meeting on Recent Advances in NMR Applications to Porous Media, Bologna, Italy*, Pergamon Press, New York (1990).

Borgia, G. C., P. Fantazzini, J. C. Gore, M. E. Smith, and J. H. Strange, eds., *Proceedings of the Second International Meeting on Recent Advances in MR Applications to Porous Media*, University of Kent at Canterbury, UK, *Pergamon Press, New York* (1993).

Borgia, G. C., P. Fantazzini, J. C. Gore, M. R. Halse, and J. H. Strange, eds., *Proceedings of the Third International Meeting on Recent Advances in {MR} Applications to Porous Media, Louvain-La-Neuve, Belgium*, Elsevier Science, New York (1996).

Box, G. E. P., *Time Series Analysis: Forecasting and Control*, Holden-Day, San Francisco (1976).

Caprihan, A., and E. Fukushima, "Flow Measurements by NMR," *Phys. Rep.* 198, 195 (1990).

Cushman, J. H., ed., *Dynamics and Fluids in Hierarchical Porous Media*, Academic Press, San Diego (1990).

Dagan, G., "A Note on Higher-Order Corrections to the Head Covariances in Steady Aquifer Flow," *Water Resour. Res.*, **21**, 573 (1985).

Dagan, G., *Flow and Transport in Porous Formation*, Springer-Verlag, New York (1989).

Dagan, G., "Higher-Order Correction of Effective Permeability of Heterogeneous Isotropic Formations of Lognormal Conductivity Distribution," *Transp. Porous Media*, **12**, 279 (1993).

Deng, F.-W., J. H. Cushman, and J. W. Delleur, "A Fast Fourier Transform Stochastic Analysis of the Contaminant Transport Problem," *Water Resour. Res.*, **29**, 3241 (1993).

Deng, F.-W., and J. H. Cushman, "On Higher-Order Corrections to the Flow Velocity Covariance Tensor, *Water Resour. Res.*, **31**, 1659 (1995).

Freyburg, D. L., "A Natural Gradient Experiment on Solute Transport in a Sand Aquifer: 2. Spatial Moments and the Advection and Dispersion of Nonreactive Tracers," *Water Resour. Res.*, **22**, 2031 (1986).

Garabedian, S. P., D. R. LeBlanc, L. W. Gelhar, and M. A. Celia, "Large-Scale Natural Gradient Tracer Test in Sand and Gravel, Cape Cod, Massachusetts. 2. Analysis of Spatial Moments for a Nonreactive Tracer," *Water Resour. Res.*, **27**, 911 (1991).

Gelhar, L. W., and C. L. Axeness, "Three-Dimensional Stochastic Analysis of Macrodispersion in Aquifiers," *Water Resour. Res.*, **19**, 161 (1983).

Gelhar, L. W., C. Welty, and K. R. Rehfeldt, "A Critical Review of Field-Scale Dispersion in Aquifiers," *Water Resour. Res.*, **28** 1955 (1992).

Greenkorn, R. A., *Flow Phenomena in Porous Media*, Dekker, New York (1983).

Hassan, A. E., "Monte Carlo Simulations of Flow and Transport in Heterogeneous Porous Media: An Evaluation of First- and Second-Order Theories and the Importance of Porosity Variability," PhD Thesis, Purdue Univ., West Lafayette, IN (1995).

Irwin, N. C., S. A. Altobelli, and R. A. Greenkorn, "Concentration and Velocity Field Measurements by Magnetic Resonance Imaging in Aperiodic Heterogeneous Porous Media," *Magn. Reson. Imaging*, **17**, 909 (1999).

Matheron, G., and G. de Marsily, "Is Transport in Porous Media Always Diffusive? A Counterexample," *Water Resour. Res.*, **16**, 901 (1980).

Nesbitt, G. J., T. W. Fens, J. S. van den Brink, and N. Roberts, "Evaluation of Fluid Displacement in Porous Media Using {NMR} Microscopy," *Magnetic Resonance Microscopy: Methods and Application in Materials Science, Agriculture, and Biomedicine*, B. Blumich and W. Kuhn, eds., VCH Publishers, New York (1992).

Smith, L., and F. W. Schwartz, "Mass Transport: 1. A Stochastic Analysis of Macroscopic Dispersion," *Water Resourc. Res.*, **16**, 303 (1980).

Sudicky, E. A., J. A. Cherry, and E. O. Frind, "Migration of Contaminants in Groundwater at a Landfill: A Case Study," *J. Hydrol*, **63**, 81 (1983).

Tompson, A. F. B., and L. W. Gelhar, "Numerical Simulation of Solute Transport in Three-Dimensional, Randomly Heterogeneous Porous Media," *Water Resour. Res.*, **26**, 2541 (1990).

Waggoner, R. A., and E. Fukushima, "Velocity Distribution of Slow Fluid Flows in Bentheimer Sandstone: An NMRI and Propagator Study," *Magn. Reson. Imaging*, **14**, 1085 (1996).

Wei, W. W. S., *Time Series Analysis: Univariate and Multivariate Methods*, Addison-Wesley, Reading, MA (1990).

Manuscript received Sept. 27, 1999, and revision received June 8, 2000.